Available online at www.sciencedirect.com
ScienceDirect
International Journal of Mass Spectrometry 268 (2007) 60–65
International Journal of Mass Spectrometry
www.elsevier.com/locate/ijms

A new apparatus for measuring rate constants and activation energies of thermal electron capture processes in the gas phase

J. Kopyra *, J. Wnorowska, M. Foryś, I. Szamrej

Chemistry Department, University of Podlasie, 08-110 Siedlce, Poland

Received 5 July 2007; received in revised form 12 August 2007; accepted 14 August 2007
Available online 19 August 2007

Abstract

The new apparatus for investigation of kinetics of a thermal electron capture process and its temperature dependence with pulsed Townsend technique has been built. This method gives straightforward results on electron drift velocities in any mixture and allows calculating the rate constants for electron capture as well as activation energies of this process. The thermal electron capture rate constants and activation energies for CH_3CCl_3, $CHCl_2CH_2Cl$ and $CH_3CHClCH_2CH_3$ have been determined.

Keywords: Pulsed Townsend technique; Halocarbon; Thermal electron capture rate constant; Activation energy

1. Introduction

The electron swarm method with an ionization chamber has been applied for many years in investigating electron attachment processes. First the dependence of an electron capture cross-section on electron energy [1] and later, after some changes of the technique, the thermal electron capture kinetics [2,3] have been investigated. This modified swarm technique, where carbon dioxide as a carrier gas was used, was very convenient, especially for studying pressure-dependent processes, e.g., Bloch–Bradbury reaction or the attachment by van der Waals dimers [4].

In all these techniques α-particles have been used as an electron swarm source [1–3].

In spite of many valuable results obtained this way, the method has its disadvantages like relatively small number of electrons produced by the α-particle, some influence of the α-particle source on the uniformity of the electric field, necessity to apply relatively high pressure and large dimension of the chamber for full absorption of the α-particle energy in the gas phase. The last made it impossible to heat and stabilize temperature to make temperature measurements.

Appearance of the fast lasers with high photon energy enabled Wang et al. [5] to apply Nd:YAG laser to produce the electron swarm which eliminates most of the above disadvantages.

The aim of this work is to apply similar technique which gives much more accurate results than electron swarm in the ionization chamber.

2. Experimental procedure

A new swarm chamber has been built for studying electron attachment processes using pulsed Townsend technique [5,6]. A schematic diagram of an experimental set up is shown in Fig. 1. It consists of a stainless steel cylindrical chamber with a volume of 700 cm^3 (1) with two stainless steel parallel electrodes (a) and (b) (6 cm in diameter, separated by 1.5 cm), a Canberra-Packard preamplifier model 2000 (2), a fast (4 ns) Tektronix oscilloscope with digital memory (3) connected with a computer (4), a computer controlled Canberra-Packard dual 0–5 kV power supply model 3125 (5), an optical set (6) and a Quantel Nd:YAG fast (5 ns) laser model Brilliant B-10 Hz (7). The laser operates on fourth harmonics at 266 nm at the frequency of 10 Hz. The pulse energy is 90 mJ. The photon energy is above the iron work function (4.5 eV [7]).

Electronically controlled heating jackets produced by Watlow Company were used to vary and stabilize the desired temperature of the chamber within 1 °C. The temperature uniformity of the

* Corresponding author. Tel.: +48 256431136.
E-mail address: kopyra@ap.siedlce.pl (J. Kopyra).

1387-3806/$ – see front matter © 2007 Elsevier B.V. All rights reserved.
doi:10.1016/j.ijms.2007.08.006

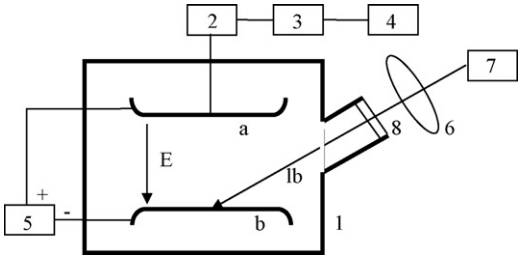

Fig. 1. Schematic diagram of the experimental set up: (1) swarm chamber, (a) anode, (b) cathode, (2) preamplifier, (3) oscilloscope, (4) personal computer, (5) high voltage power supplier, (6) optical set up, (7) laser, and (8) quartz window. lb, laser light; E, uniform electric field.

chamber is monitored with four thermocouples around and one inside the chamber.

The laser beam lb going through the optics is focused by converging lens (6) and further enters the chamber (1) through a quartz window (8) and strikes the center of the cathode (b). The generated electrons drift toward the anode under the influence of the uniform electric field (E) created by power supply (5). In the presence of carbon dioxide which is used as a carrier gas they are immediately thermalized. This comes from the fact that electron mobility does not depend on E/N in the whole range of the used E/N values (up to 1×10^{-17} V cm^2 molec.$^{-1}$) as we have demonstrated it in Ref. [2].

Traversing electrons induce the change of the anode potential which increases linearly as electrons move to the collecting electrode in the pure buffer gas. In the mixture of electron scavenger and buffer gas the electrons are captured by the scavenging gas and increase in the potential is no longer linear. The output signal is amplified by preamplifier, registered on an oscilloscope and saved in a computer memory. The method offers the opportunity to obtain a drift velocity and an electron attachment rate constant independently. The drift velocity, W, is equal to the quotient of the distance traversed by electrons to the collecting electrode, d, and the drift time, t_0, i.e., the time when electron swarm reaches the anode ($W = d/t_0$). Fig. 2 shows the pulse which is the result

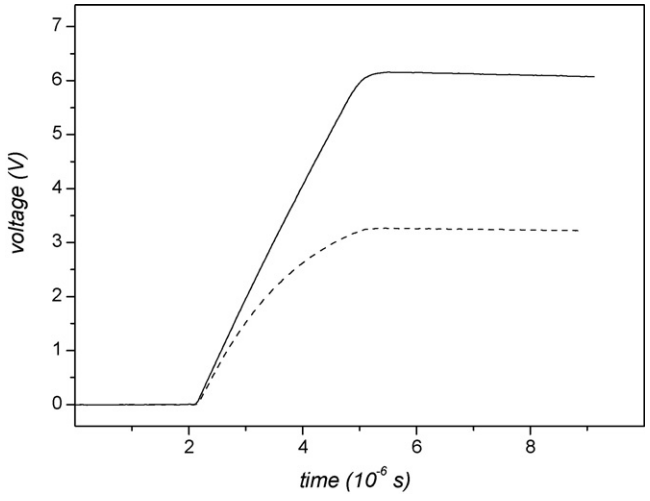

Fig. 2. Averaged voltage signal for the pure CO_2 (solid line) and the mixture of $CHCl_2CH_2Cl$ and CO_2 (dotted line) obtained at 298 K and $E/N = 3$ Td (1 Td = 10^{-17} V cm^2 molec.$^{-1}$).

of averaging of the 100 consecutive pulses. The electron attachment rate constant can be determined from the shape of the output signal of the electron pulse.

During the electron attachment process negative ions are produced (e.g., Cl^-) which also move to the anode. However owing to their large mass in comparison with that of electron they drift ca. 300 times slower and do not influence the electrode potential during electrons drift time as it was experimentally demonstrated by Wang et al. [5]. Therefore we will not include them in further consideration.

The change in electrode potential U caused by drifting electrons during a time dt is proportional to an actual number of electrons, N_e, at a given time t and the distance from anode. The last can be expressed as the ratio of the actual time t and drift time t_0, t/t_0. Thus:

$$dU(t) = \frac{a' N_e \, dt}{t_0} \quad \text{(I)}$$

where a' is a coefficient of proportionality. In the case of non-attaching gas $N_e = N_e^0$—the number of electrons produced by a laser pulse and $U(t)$ is a linear function of t:

$$U(t) = \frac{a' N_e^0 t}{t_0} \quad \text{(II)}$$

The number of electrons removed by electron scavenger during the time dt is proportional to an actual number of electrons and a number density of the electron scavenger, N_a:

$$dN_e = -kN_e N_a \, dt \quad \text{(III)}$$

After integrating we have:

$$N_e = N_e^0 \exp(-kN_a t) \quad \text{(IV)}$$

Introducing expression (IV) into Eq. (I) we obtain:

$$dU(t) = \frac{a' N_e^0 \exp(-kN_a t) \, dt}{t_0} \quad \text{(V)}$$

Integrating Eq. (V) in the range from 0 to U and from 0 to t we get the temporal variation of the anode potential, $U(t)$, due to the drift of the electron swarm ($t \leq t_0$) in the presence of electron scavenger, Eq. (VI):

$$U(t) = \frac{a' N_e^0}{kN_a t_0}[1 - \exp(-kN_a t)] \quad \text{(VI)}$$

As N_e^0 is a constant value, we can write $a = a' N_e^0$ and eventually:

$$U(t) = \frac{a}{kN_a t_0}[1 - \exp(-kN_a t)] \quad \text{(VII)}$$

As the laser pulse time, the response time of the oscilloscope and response time of the preamplifier to the change in potential (20 ns) are much shorter than the electron swarm drift time (a few μs), they do not influence the pulse shape. The decay function of the preamplifier (for any time t) is given by Eq. (VIII):

$$G(t) = b \exp\left(-\frac{t}{t_1}\right) \quad \text{(VIII)}$$

where b is a coefficient of proportionality and $t_1 = RC$ is a time constant (R is the input resistance of the preamplifier and C is the overall capacitance of the anode circuit) equal to 400 μs as calculated from the shape both of rectangular pulse generator and the curve in Fig. 2 for the time $t > t_0$. As it can slightly influence the shape of the pulse it should be taken into account. The value of the output potential of the preamplifier during a time $\tau \leq t_0$, $V(\tau)$, is a result of both processes occurring simultaneously:

$$V(\tau) = \int_0^{\tau} \frac{\mathrm{d}U(t)}{\mathrm{d}t} G(\tau - t)\,\mathrm{d}t \qquad \text{(IX)}$$

Eqs. (VII)–(IX) were first introduced by Christophorou (cf. [8]) and used by us in Ref. [3].

Solution of the integral in Eq. (IX) is as follows:

$$V(\tau) = \frac{At_1}{t_0(1 - kN_a t_1)} \left[\exp(-kN_a\tau) - \exp\left(\frac{-\tau}{t_1}\right)\right] \qquad \text{(X)}$$

The experimental curves as shown in Fig. 2 were fitted using Eq. (X) with Simplex and χ^2 algorithms which gave the same results.

As is easily seen from Eq. (X), (1) the constant $A = ab$ has a dimension of volts, (2) for a given curve the expression before square brackets contains only constants and effectively is simulated by computer as one arbitrary constant, and (3) as τ/t_1 ratio in second exponent does not exceed 1–2%, this exponent only slightly influences the whole expression in square brackets. Thus, while we use full Eq. (X), the effective unambiguous task of the fitting program is to find some arbitrary constant B and the electron capture rate constant k in equation of the type of Eq. (XI):

$$V(\tau) = B\exp(-kN_a\tau) \qquad \text{(XI)}$$

After the electron swarm arrives at the anode the potential decreases exponentially through RC. As t_0 is of the order of a few μs, $t_1 \gg t_0$ and decay only slightly influences the change in potential during drift time. The resulting voltage signal without and with electron scavenger is shown in Fig. 2. As can be seen, owing to high energy of laser pulse the change in potential is rather high (a few V), much higher than an electronic noise (a few mV).

The shape of the pulse in principle can be deformed by the longitudinal diffusion of electrons during the drift of the swarm. The deformation is generally thought to be negligible. This can be justified using Eq. (XII) introduced by Hunter and Christophorou [9]:

$$\frac{D_L}{\mu} = \frac{V(\delta t)^2}{4t_0^2} \qquad \text{(XII)}$$

where D_L/μ is the ratio of a longitudinal diffusion coefficient, D_L, to electron mobility, μ ($=W/(E/N)$), V the potential applied cross the drift gap, δt the half-width of an electron swarm profile and t_0 is the drift time. In our experiments V is in the range 70–130 V, t_0 is 4 μs and $D_L/\mu = 0.03$ V for CO_2 in the range of applied E/N [9] which gives the ratio $\delta t/t_0$ less than a few percent at the lowest applied potential. Therefore widening the electron swarm due to diffusion can be neglected. Since in our range of E/N (where electrons are in thermal distribution with gas molecules) a transverse diffusion coefficient is equal to longitudinal diffusion coefficient [9], the effect of the transverse diffusion is negligible as well.

From the Nernst–Townsend relation, Eq. (XIII) (cf. [9]), the influence of temperature on the thermal diffusion coefficients, D ($D_L = D_T$ in thermal conditions) can be derived:

$$\frac{W}{D} = \frac{eE}{kT} \qquad \text{(XIII)}$$

As the temperature change in this experiment is not more than 30% its influence on the pulse shape can also be neglected.

CH_3CCl_3, $CHCl_2CH_2Cl$ and $CH_3CHClCH_2CH_3$ were provided by Sigma Aldrich Co. with a purity of 99.8, 97 and 99.9%, respectively. CO_2 with a quoted purity 99.998% was from Fluka and used as delivered. The applied pressure of the electron attaching gases depends on their efficiency in attaching electrons and is chosen to give the rate of the process approximately 10^5 s^{-1}. The total pressures of the gas mixtures were in the range 100–130 Torr (1 Torr = 133.3 Pa) and was controlled by an absolute pressure transducer (MKS Baratron 116A) with an accuracy of 1 mTorr. If the chosen pressure of the attaching gas was in the range of mTorr (or less), its more concentrated mixture (at least 1 Torr) with CO_2 has been prepared. Then proper amount of it was introduced into the chamber.

The overall accuracy of the experiment should be much better than with ionization chamber for several reasons:

1. Elimination of the α-source ensures a full uniformity of the electric field between electrodes.
2. Owing to high laser pulse energy the number of produced electrons is much higher and the preamplifier output signal is in the range of volts while from ionization chamber it was of the order of tens of mV at electronic noise of a few mV.
3. Owing to the heating system we can make the experiment at well-defined temperature (within 1 °C), not just the "room temperature". It is easy to calculate, that if one increases the "room temperature" from 18 to 25 °C the rate constant at activation energy of 0.3 eV changes by 30% and at activation energy of 0.5 eV even by 60%.

3. Results and discussion

Introducing the new method of measurement we have repeated an experiment at room temperature for some previously measured systems to check its reliability. As it can be seen from Table 1, the higher the rate constant the better the agreement between results. It is quite understandable if we take into account the role of impurities in the measurements of the attachment process. We try to purify our compounds carefully applying freeze–pump–thaw technique using different freezing mixtures and purifying compounds both from higher and lower volatile impurities. But still for the molecules with very low rate constant of electron attachment even the very small traces (of the order of ppm) of the impurity with very high rate constant (e.g., CCl_4, $CHCl_3$) have a great influence on the measured value.

Table 1
The comparison of the room temperature (298 K) thermal electron capture rate constants obtained with electron swarm method in ionization chamber and the present one

Molecule	k_{th} (cm^3 $molec.^{-1}$ s^{-1})	
	Ionization chamber	Present results
SF_6	$(2.5 \pm 0.3) \times 10^{-7}$ [2]	$(2.5 \pm 0.2) \times 10^{-7}$
$CH_2ClCH_2CH_2Cl$	$(2.0 \pm 0.3) \times 10^{-12}$ [10]	$(1.4 \pm 0.1) \times 10^{-12}$
CH_3CF_2Cl	$(6.0 \pm 0.9) \times 10^{-13}$ [10]	$(4.8 \pm 0.4) \times 10^{-13}$

For the first measurements at different temperatures we have chosen two trichloroethane isomers. The average literature rate constants for them are quite high and differ by two orders of magnitude (1.4×10^{-8} and 2×10^{-10} cm^3 $molec.^{-1}$ s^{-1} for CH_3CCl_3 and $CHCl_2CH_2Cl$, respectively [10]).

In the case of both compounds the attachment process is simple two-body reaction:

$$e^- + RCl \rightarrow R + Cl^- \quad \text{(XIV)}$$

We have measured thermal electron capture rate constants (k_{th}) in the temperature range 298–373 K for CH_3CCl_3. In the case of $CHCl_2CH_2Cl$ this range was much narrower (298–343 K), however, sufficient to obtain the activation energy of the process. The experimental results are presented in Fig. 3(a) and (b). At the lowest temperature of 298 K (room temperature) we have obtained the rate constants 3.8×10^{-8} and 3.7×10^{-10} cm^3 $molec.^{-1}$ s^{-1} for CH_3CCl_3 and $CHCl_2CH_2Cl$, respectively. In both cases we observed the increase in k_{th} with temperature which shows that the investigated processes require some activation energies. They can be calculated from the Arrhenius equation:

$$\ln(k) = A - \frac{E_a}{k_B T} \quad \text{(XV)}$$

where A is a pre-exponential factor, E_a the activation energy and k_B is the Boltzmann constant.

In Fig. 4 the Arrhenius plots are presented. From their slopes the activation energy can be derived. It is equal to 0.09 and 0.16 eV for CH_3CCl_3 and $CHCl_2CH_2Cl$, respectively.

To demonstrate the influence of the impurity on the measurements of the attachment process and the important role of simultaneous measurements of both rate constant and activation energy we will present the results we have obtained for $CH_3CHClCH_2CH_3$.

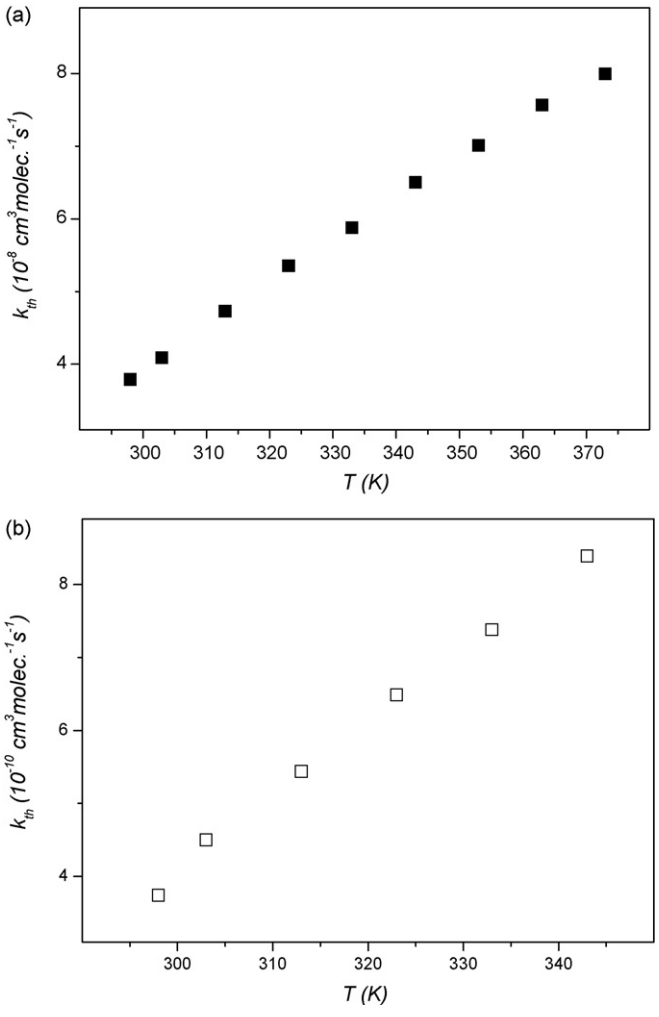

Fig. 3. The dependence of thermal electron capture rate constant on temperature for (a) CH_3CCl_3 and (b) $CHCl_2CH_2Cl$.

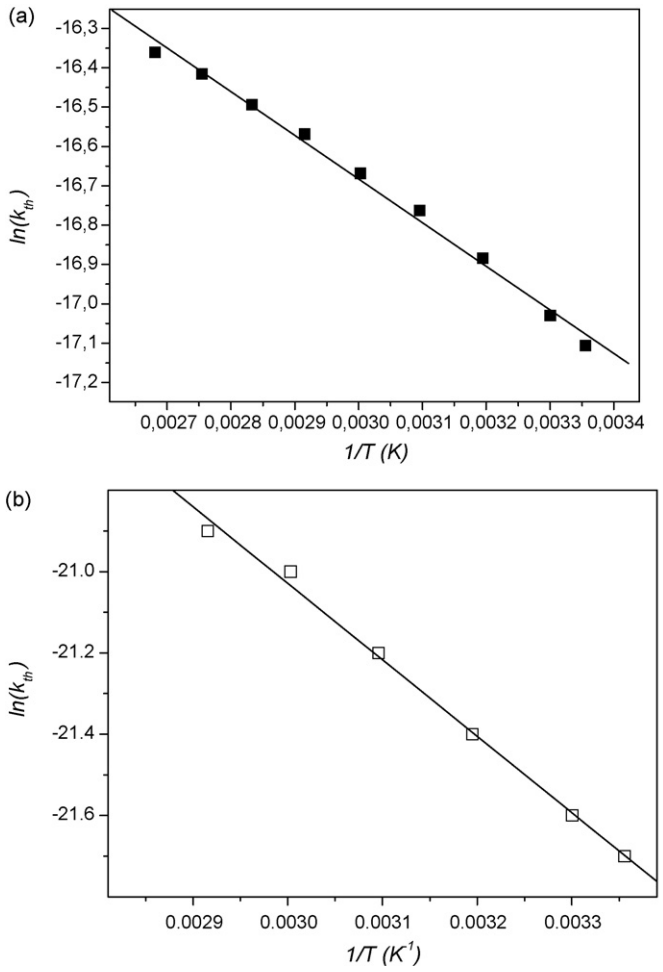

Fig. 4. Arrhenius plot for (a) CH_3CCl_3 and (b) $CHCl_2CH_2Cl$.

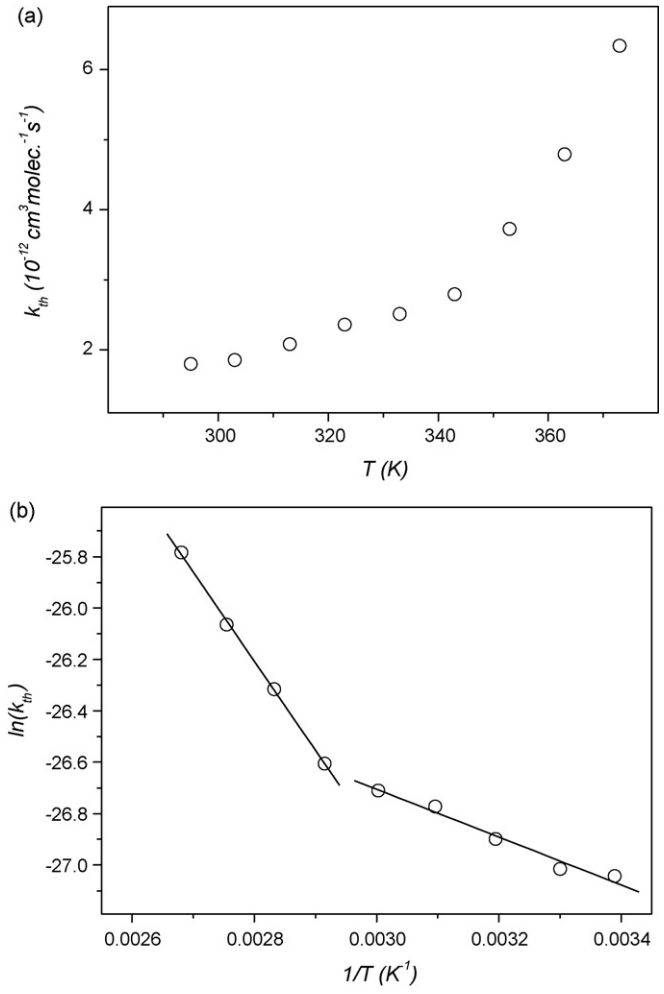

Fig. 5. The dependence of (a) k_{th} on T and (b) ln(k_{th}) on $1/T$ for $CH_3CHClCH_2CH_3$ (after purification using freeze–pump–thaw technique, see text).

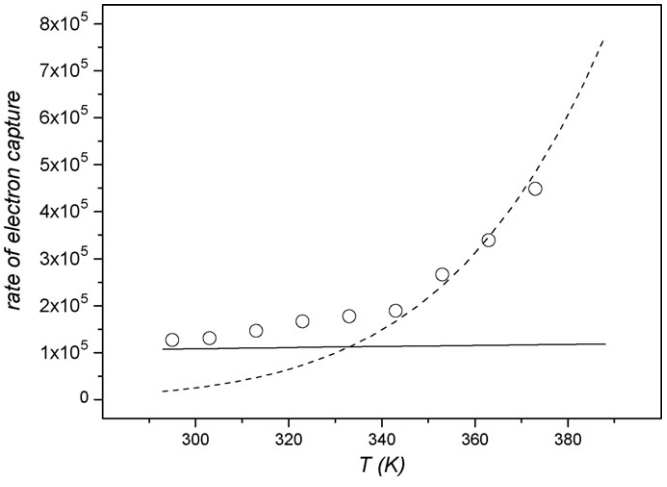

Fig. 6. The effect of impurity on the electron capture rate: solid line, the calculations for impurities; dotted line, the calculations for pure compound; ◯, experimental results (for details see text).

The room temperature rate constant for the electron attachment by this molecule, after careful purification, using freeze–pump–thaw technique, of the sample was equal to 1×10^{-12} cm^3 molec.$^{-1}$ s^{-1}. Comparing it with the literature value for $CH_3CHClCH_3$ which is equal to 3.8×10^{-12} cm^3 molec.$^{-1}$ s^{-1} (3.6×10^{-13} cm^3 molec.$^{-1}$ s^{-1} for $CH_2ClCH_2CH_3$) [10] the obtained value seems quite reasonable. But the influence of temperature on this rate constant is difficult to explain. In Fig. 5(a) and (b) the dependences of k_{th} on T and ln(k_{th}) on $1/T$ for $CH_3CHClCH_2CH_3$ are plotted. There are two different slopes—one for lower (up to 340 K) and other one for higher temperatures. The only explanation for such results is the contribution of a low concentration of impurity which was not removed with the applied purification procedure. It should accept electrons with high rate constant and low activation energy.

To show the effect of impurity we have made the following simulation. We have calculated, according to Arrhenius equation, the temperature dependence of the rate of the electron capture process for the molecule with concentration of 3×10^{17} molec. cm^{-3} (the concentration of $CH_3CHClCH_2CH_3$ we have used in the experiment) which attach electrons with

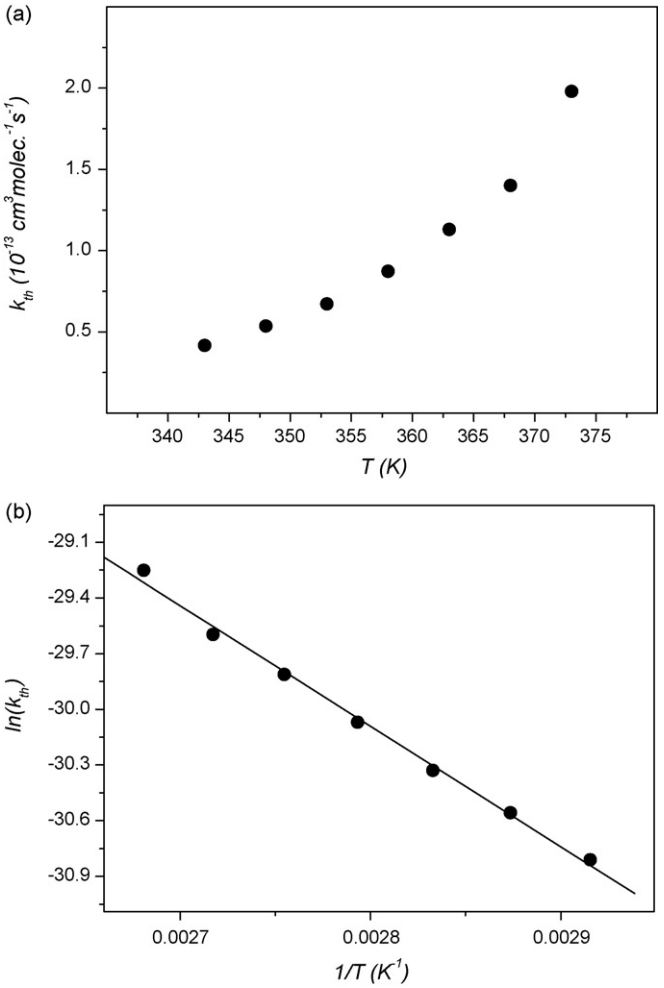

Fig. 7. The dependence of (a) k_{th} on T and (b) ln(k_{th}) on $1/T$ for $CH_3CHClCH_2CH_3$ (after fractional distillation, see text).

Table 2
Thermal electron attachment rate constants (298 K) and activation energies calculated from kinetic data for chloroalkanes

Molecule	k_{th} (cm^3 molec.$^{-1}$ s^{-1})[a]	E_a (eV) [11]
CH_3Cl	2.0×10^{-13}, $<1 \times 10^{-16}$ [13][b]	0.48
CH_2Cl_2	4.7×10^{-12}	0.29
$CHCl_3$	2.7×10^{-9}, 4.4×10^{-9} [12]	0.12, 0.12 [12]
CCl_4	4.0×10^{-7}	0
CH_3CHCl_2	2.1×10^{-11}	0.25
CH_2ClCH_2Cl	2.9×10^{-11}	0.24
CH_3CCl_3	1.4×10^{-8}, 1.5×10^{-8} [12], 3.8×10^{-8}[c]	0.16, 0.13 [12], 0.09[c]
$CHCl_2CH_2Cl$	3.1×10^{-10} [12], 3.7×10^{-10}[c]	0.2 [12], 0.16[c]
$CH_3CHClCH_2CH_3$	2.0×10^{-15}[c]	0.55[c]

[a] Averaged data from Table 1 in [10].
[b] Theoretical data from semiempirical calculations of DA.
[c] Present data.

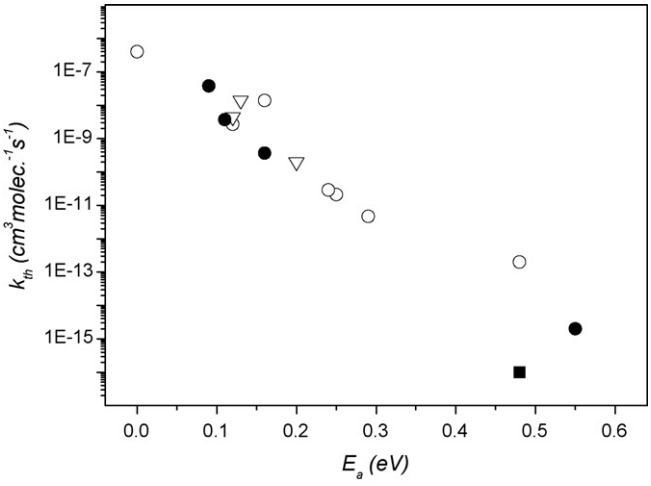

Fig. 8. The room temperature thermal electron capture rate constants as a function of the activation energies for some chloroalkanes: (●) present results; (▽) data from [12]; (◯) other data from Table 2; (■) theoretical data from [13].

the rate constant 1×10^{-13} cm^3 molec.$^{-1}$ s^{-1} and the activation energy of 0.5 eV (E_a for similar compounds [11]). The same calculations were performed for the impurity molecule with concentration 3×10^{11} molec. cm^{-3} attaching electrons with the rate constant of 4×10^{-7} cm^3 molec.$^{-1}$ s^{-1} and activation energy equal to 0 eV. The results of the simulation are shown in Fig. 6. If the mixture of such two compounds is measured up to 330–340 K the attachment is caused mostly by the impurity. As one can see our experimental data fit to this picture.

Because usually used method of purification was not efficient enough to get rid of small concentration of impurities we have applied fractional distillation with a bubble-cap column. The results we have got after this procedure are presented in Fig. 7.

As it is seen from Fig. 7(a), the measurements have been started at the temperature 343 K as there was no visible attachment at lower temperatures. The obtained activation energy is equal to 0.55 eV (Fig. 7(b)) and the rate constant extrapolated to room temperature is 2×10^{-15} cm^3 molec.$^{-1}$ s^{-1}.

Finally, let us compare the relationship between the room temperature thermal electron capture rate constants and the activation energies for a number of chloroalkanes. In Table 2 the available literature and present data are demonstrated. Fig. 8 shows the plot of log(k_{th}) versus E_a. As one should expect there is a straightforward linear dependence between logarithm of the rate constant and activation energy for the attachment process. Looking back to our first results for $CH_3CHClCH_2CH_3$ and the analysis we have made for it the only way to check the reliability of the electron attachment rate constants is to measure simultaneously the temperature effect on it.

4. Conclusions

1. The new electron swarm apparatus has been built which allows measuring the electron capture rate constants up to 470 K.
2. New results on rate constants and activation energies have been obtained.
3. A necessity to determine simultaneously both rate constant and activation energy has been demonstrated.

Acknowledgment

This research was supported from Polish scientific funds for the years 2005–2008 under Grant 3 T09A 111 29.

References

[1] D.L. McCorkle, I. Szamrej, L.G. Christophorou, J. Chem. Phys. 77 (1982) 5542.
[2] I. Szamrej, M. Foryś, Radiat. Phys. Chem. 33 (1989) 393.
[3] A. Rosa, W. Barszczewska, M. Foryś, I. Szamrej, Int. J. Mass Spectrom. 205 (2001) 85.
[4] I. Szamrej, M. Foryś, Prog. React. Kinet. 23 (1998) 117.
[5] Y. Wang, L.G. Christophorou, J.K. Verbrugge, J. Chem. Phys. 109 (1998) 8304.
[6] J. deUrquijo, C.A. Arriaga, C. Cisneros, I. Alvarez, J. Phys. D: Appl. Phys. 32 (1999) 41.
[7] CRC Handbook of Chemistry and Physics, 73rd ed., CRC Press, Boca Raton, FL, 1992–1993.
[8] L.G. Christophorou, Atomic and Molecular Radiation Physics, John Wiley and Sons, New York, 1971, p. 442.
[9] S.R. Hunter, L.G. Christophorou, in: L.G. Christophorou (Ed.), Electron Molecule Interactions and Their Applications, vol. 2, Academic Press, New York, 1984.
[10] W. Barszczewska, J. Kopyra, J. Wnorowska, I. Szamrej, J. Phys. Chem. A 107 (2003) 11427.
[11] E.C.M. Chen, E.S. Chen, The Electron Capture Detector and The Study of Reactions with Thermal Electrons, John Wiley and Sons, New Jersey, 2004, p. 272, E_a calculated from kinetic data.
[12] D. Smith, P. Spanel, Adv. Atom. Mol. Opt. Phys. 32 (1994) 307.
[13] I.I. Fabrikant, J. Phys. B 24 (1991) 2213.